Elastic decomposition with downhole geophones and hydrophones

Joost van der Neut[1], Nihed El Allouche[1] and Kees Wapenaar[1],*
[1]Delft University of Technology, Department of Geotechnology.

Summary
Decomposition of elastic wavefields into downgoing and upgoing P- and S-wave modes requires knowledge of particle velocity and traction across a receiver array. For land data, receivers are generally deployed at the earth's surface where traction components vanish, such that decomposition can be obtained with solely multi-component geophones. For Ocean-Bottom-Cable data, receivers are deployed at the seafloor where shear traction components vanish but normal traction components do not, such that an additional hydrophone is required to allow complete decomposition of the elastic system. Receivers can also be deployed in boreholes. In this environment, none of the traction components vanish, such that elastic decomposition requires knowledge of both the particle velocity and traction vector across the receiver array. Downhole geophones and hydrophones can be deployed, recording particle velocity and pressure (normal traction), but the shear traction is generally not recorded, making the elastic decomposition problem underdetermined. To solve this we introduce an additional constraint by separating up- and downgoing S-waves with time-gates and incorporating them in the elastic decomposition scheme.

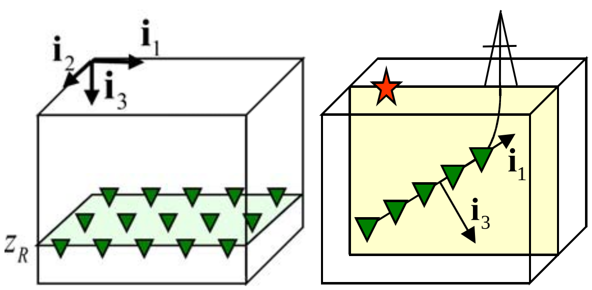

Fig 1a: Ideal configuration for elastic decomposition at a horizontal receiver level at depth $x_3 = z_R$ in a Cartesian coordinate system spanned by normal vectors $\mathbf{i}_1$, $\mathbf{i}_2$ and $\mathbf{i}_3$; b) Configuration for downhole elastic decomposition in a plane spanned by the source location and the well with receivers, where $\mathbf{i}_1$ and $\mathbf{i}_3$ are chosen parallel and perpendicular to the well.

Introduction

Various geophysical methods that deploy downhole receivers would benefit from the separation of observed wavefields in upgoing and downgoing P- and S-wave modes. A good example is the virtual source method, where downhole receivers are transformed into virtual sources through a cross-correlation procedure (Bakulin and Calvert, 2006). Mehta et al. (2007) showed that decomposing the up- and downgoing wavefields can improve the quality of virtual source data significantly. Other advancing technologies for virtual source processing, such as multi-dimensional deconvolution (Wapenaar et al., 2008), even fully depend on such decomposition.

To illustrate elastic decomposition in general, we define a 3D Cartesian coordinate system $\mathbf{x} = x_1\mathbf{i}_1 + x_2\mathbf{i}_2 + x_3\mathbf{i}_3$, with a 2D receiver array at fixed depth $x_3 = z_R$, see Figure 1a. The elastic wavefield at the receiver level can be fully described by the 3-component particle velocity vector $\mathbf{v} = (v_1, v_2, v_3)^T$ and a 3-component vector of tractions acting across the receiver array $\boldsymbol{\tau}_3 = (\tau_{13}, \tau_{23}, \tau_{33})^T$, where superscript T denotes the transpose. These vectors can be combined in the two-way wave vector . If $\mathbf{Q} = (\{-\boldsymbol{\tau}\}^T, \{\mathbf{v}\}^T)^T$ is well sampled throughout the receiver array and medium properties are approximately constant at z_R, elastic decomposition can be performed in the (ω, k_1, k_2)-domain, where ω is the angular frequency and k_α is the wavenumber in the $\mathbf{i}_\alpha$-direction. We indicate this domain with a tilde. $\tilde{\mathbf{Q}}$ can now be decomposed by inverting a matrix relation $\tilde{\mathbf{Q}} = \tilde{\mathbf{L}}\tilde{\mathbf{P}}$ (Woodhouse, 1974; Wapenaar and Berkhout, 1989), where $\tilde{\mathbf{L}}$ is a composition matrix depending on the medium parameters at the receiver level and $\tilde{\mathbf{P}} = (\{\tilde{\mathbf{P}}^+\}^T, \{\tilde{\mathbf{P}}^-\}^T)^T$, where $\tilde{\mathbf{P}}^+$ and $\tilde{\mathbf{P}}^-$ are vectors containing the downgoing and upgoing wavefields, each consisting of P-, SV- and SH-components.

In elastic media, $\tilde{\mathbf{Q}}$ and $\tilde{\mathbf{P}}$ are 6-dimensional. Full elastic decomposition thus requires the installation of 6 independent receiver components. For land data, acquisition is generally performed at the free surface, such that the traction vector vanishes. This allows us to decompose wavefields with 3-component geophones only (Dankbaar, 1985; Wapenaar et al., 1990; Robertsson and Curtis, 2002). If receivers are located at a seafloor, the shear traction components $\tilde{\tau}_{13}$ and $\tilde{\tau}_{23}$ vanish, but the normal traction component $\tilde{\tau}_{33}$ does not. By obtaining measurements of the particle velocity vector and the acoustic pressure (which can be related to $-\tilde{\tau}_{33}$), elastic decomposition can also be applied in this environment (Amundsen and Reitan, 1995; Schalkwijk et al., 2003; Muijs et al., 2007).

For decomposition in boreholes we are not that fortunate, since none of the components of $\tilde{\mathbf{Q}}$ vanishes. This means that theoretically 6-component data is required to perform elastic decomposition. In practice we measure at most 4 components, namely the particle velocity vector and pressure. Moreover, full 3D decomposition requires receivers in a 2D array (Figure 1a), whereas in practice downhole receivers are only sampled in the direction of the well trajectory, see Figure 1b.

Theory

Since downhole receivers only sample the wavefield in one spatial direction, we reduce the spatial dimensions of our problem. We define a 2D plane containing the well and the source location, see Figure 1b. Wave propagation outside this plane is neglected, reducing our number of spatial dimensions from 3 to 2. A Cartesian coordinate system is defined in the propagation plane with normal vectors $\mathbf{i}_1$ parallel to the well and $\mathbf{i}_3$ perpendicular to the well. In various decomposition schemes, up- and downgoing P- and S-waves are separated with respect to the $\mathbf{i}_1$ direction (parallel to the well), where the downward direction is $+\mathbf{i}_1$ and the upward direction is $-\mathbf{i}_1$ (Leaney, 1990; Sun et al., 2009). However, in this paper, we apply decomposition with respect to the $\mathbf{i}_3$ direction (perpendicular to the well). In this case, the downward direction is $+\mathbf{i}_3$ and the upward direction is $-\mathbf{i}_3$. This is especially useful for horizontal or near-horizontal wells, as often considered in the virtual source method (Bakulin and Calvert, 2006). Under this definition, full decomposition would require a 4-component vector $\mathbf{Q}$, consisting of 2-component particle velocity vector $\mathbf{v}=(v_1,v_3)^T$ and 2-component traction vector $\boldsymbol{\tau}_3=(\tau_{13},\tau_{33})^T$. If such measurements would be available, we could set up the composition equation $\tilde{\mathbf{Q}}=\tilde{\mathbf{L}}\tilde{\mathbf{P}}$, which we write as

$$\begin{pmatrix} -\tilde{\tau}_{13} \\ -\tilde{\tau}_{33} \\ \tilde{v}_1 \\ \tilde{v}_3 \end{pmatrix} = \begin{pmatrix} \tilde{L}^+_{1,11} & \tilde{L}^+_{1,12} & \tilde{L}^-_{1,11} & \tilde{L}^-_{1,12} \\ \tilde{L}^+_{1,21} & \tilde{L}^+_{1,22} & \tilde{L}^-_{1,21} & \tilde{L}^-_{1,22} \\ \tilde{L}^+_{2,11} & \tilde{L}^+_{2,12} & \tilde{L}^-_{2,11} & \tilde{L}^-_{2,12} \\ \tilde{L}^+_{2,21} & \tilde{L}^+_{2,22} & \tilde{L}^-_{2,21} & \tilde{L}^-_{2,22} \end{pmatrix} \begin{pmatrix} \tilde{P}^+_P \\ \tilde{P}^+_S \\ \tilde{P}^-_P \\ \tilde{P}^-_S \end{pmatrix}, \tag{1}$$

Some freedom exists in scaling the composition matrix $\tilde{\mathbf{L}}$, depending on what we want the decomposed field to represent. Here we choose to impose flux-normalization, meaning that the power-flux of the two-way wavefield $-\tilde{\boldsymbol{\tau}}_3^\dagger\tilde{\mathbf{v}}-\tilde{\mathbf{v}}^\dagger\tilde{\boldsymbol{\tau}}_3$ equals the power-flux of the decomposed wavefield $\{\tilde{\mathbf{P}}^+\}^\dagger\tilde{\mathbf{P}}^+-\{\tilde{\mathbf{P}}^-\}^\dagger\tilde{\mathbf{P}}^-$ (Frasier, 1970), which allows us to derive one-way reciprocity theorems (Wapenaar et al., 2001). An exact representation of $\tilde{\mathbf{L}}$ obeying power-flux normalization is given by e.g. Ursin (1983) and Wapenaar et al. (2008). For many applications, such as the virtual source method (Bakulin and Calvert, 2006), wave propagation is often close to normal incidence with respect to the well. At normal incidence, it is well known that the decomposition system uncouples since various elements of $\tilde{\mathbf{L}}$ vanish such that equation 1 can be rewritten as

$$\begin{pmatrix} -\tilde{\tau}_{13} \\ -\tilde{\tau}_{33} \\ \tilde{v}_1 \\ \tilde{v}_3 \end{pmatrix} = \begin{pmatrix} 0 & \tilde{L}^+_{1,12} & 0 & \tilde{L}^-_{1,12} \\ \tilde{L}^+_{1,21} & 0 & \tilde{L}^-_{1,21} & 0 \\ 0 & \tilde{L}^+_{2,12} & 0 & \tilde{L}^-_{2,12} \\ \tilde{L}^+_{2,21} & 0 & \tilde{L}^-_{2,21} & 0 \end{pmatrix} \begin{pmatrix} \tilde{P}^+_P \\ \tilde{P}^+_S \\ \tilde{P}^-_P \\ \tilde{P}^-_S \end{pmatrix}. \tag{2}$$

In this special case, up- and downgoing P-waves can be described by $\tilde{\tau}_{33}$ and $\tilde{v}_3$ solely and up- and downgoing S-waves can be described by $\tilde{\tau}_{13}$ and $\tilde{v}_1$ solely. This fact is exploited in the well-known dual sensor approach, where the P-wave system is decomposed by summing or adding weighted contributions of $\tilde{\tau}_{33}$ and $\tilde{v}_3$, assuming near-normal incidence propagation (Barr, 1997; Mehta et al., 2009). As mentioned before, the shear traction component $\tilde{\tau}_{13}$ is generally not recorded by downhole receivers. This leaves us with an underdetermined system of 3 equations and 4 unknowns. To overcome this problem, we introduce an additional constraint by replacing $\tilde{\tau}_{13}$ and the first row in matrix $\tilde{\mathbf{L}}$ with coefficients $\tilde{A}$, $\tilde{C}^\pm_P$ and $\tilde{C}^\pm_S$:

$$\begin{pmatrix} \tilde{A} \\ -\tilde{\tau}_{33} \\ \tilde{v}_1 \\ \tilde{v}_3 \end{pmatrix} = \begin{pmatrix} \tilde{C}^+_P & \tilde{C}^+_S & \tilde{C}^-_P & \tilde{C}^-_S \\ \tilde{L}^+_{1,21} & \tilde{L}^+_{1,22} & \tilde{L}^-_{1,21} & \tilde{L}^-_{1,22} \\ \tilde{L}^+_{2,11} & \tilde{L}^+_{2,12} & \tilde{L}^-_{2,11} & \tilde{L}^-_{2,12} \\ \tilde{L}^+_{2,21} & \tilde{L}^+_{2,22} & \tilde{L}^-_{2,21} & \tilde{L}^-_{2,22} \end{pmatrix} \begin{pmatrix} \tilde{P}^+_P \\ \tilde{P}^+_S \\ \tilde{P}^-_P \\ \tilde{P}^-_S \end{pmatrix}. \tag{3}$$

Since $\tilde{\tau}_{13}$ is not recorded, separation of up- and downgoing S-waves is impossible at normal incidence. As many practical applications require good separation near or close to normal incidence, our constraint should in some way introduce the separation of up- and downgoing S-waves to the decomposition system. We notice that upgoing S-waves generally arrive relatively late with respect to the other components. For early arrival times, a reasonable assumption seems that no upgoing S-waves exist, in other words: $\tilde{P}^-_S=0$. This assumption can be introduced in equation 3 by the coefficients defined in Table 1, yielding a system of 4 equations and 4 unknowns which can be inverted. It is our experience that the $\tilde{P}^-_S=0$-assumption allows us to discriminate well between up- and downgoing P-waves throughout the gathers. For S-waves, we have to adopt a different strategy.

assumption	$\tilde{A}$	$\tilde{C}_P^+$	$\tilde{C}_S^+$	$\tilde{C}_P^-$	$\tilde{C}_S^-$
$\tilde{P}_S^- = 0$	0	0	0	0	1
$\tilde{P}_S^+ = 0$	0	0	1	0	0

Table 1: Coefficients for different assumptions.

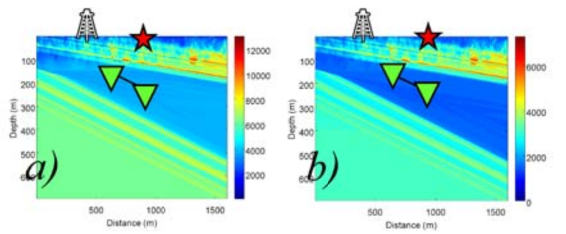

Fig 2: Model of a) P-wave impedance and b) S-wave impedance with the source (red) and receivers (green) in a deviated well.

The first significant upgoing S-wavefield can often be distinguished by visual inspection. We place a time-gate right above this event. For the 'upper' part (meaning early arrival times) of the data, we adapt the $\tilde{P}_S^- = 0$-assumption to retrieve the downgoing S-wavefields. For the 'lower' part (meaning late arrival times) of the data, we assume that no downgoing S-wave is present, which is imposed by a $\tilde{P}_S^+ = 0$-assumption, introduced by the coefficients as given in Table 1. It should be noted that downgoing S-waves will often exist in the lower part, especially stemming from interactions with the free surface (multiples). For the model we considered, the $\tilde{P}_S^+ = 0$-assumption appeared relatively successful in extracting the dominant upgoing S-wave. For different data sets, alternative constraints may be preferred.

Synthetic example

In Figure 2 we show a 2D elastic synthetic model, based on a real field of Shell in the Middle East. 128 multi-component receivers are located in a deviated well below the source location. The overburden has a complicated nature, causing distorted wavefields once they arrive at the receiver level (Korneev et al., 2009). In Figure 3 we show the recorded data from a horizontal force source after gain correction to amplify the late arrivals. First we applied elastic decomposition using all receiver components, yielding the gathers as shown in Figure 4. Note that downgoing S-waves have leaked into the upgoing S-wave gather, since the assumption that medium parameters are constant at the receiver level was only approximately fulfilled. Next we applied decomposition without shear traction by adopting the $\tilde{P}_S^- = 0$-assumption. In Figures 5a and 5b we show the retrieved downgoing and upgoing P-wavefield using this approach. Note the close match with the decomposed fields in Figures 4a and 4b. Also the downgoing S-wave (Figure 5c) is retrieved relatively well by the modified scheme (compared to Figure 4c). We placed a time gate (green dashed line) below the first significant upoing S-wave and muted all information below. For later times, we adopted the $\tilde{P}_S^+ = 0$-assumption to retrieve the upgoing S-wavefield, see Figure 5d. Note that this field is not as accurately retrieved as in Figure 4d, due to the missing shear traction. The introduced noise is mainly caused by downgoing S-waves leaking into the upgoing S-wave gather.

Next we replace the horizontal force source with a vertical force source. Input data and results from the full decomposition scheme are shown in Figures 6 and 7. The up- and downgoing P-waves as well as the downgoing S-waves can be accurately retrieved with the $\tilde{P}_S^- = 0$-assumption, as demonstrated in Figures 8a, 8b and 8c. The upgoing S-waves in Figure 7d mainly stem from converted P-waves. These waves are relatively weak and not visible in the original data (Figure 6). If we place a time-gate right above these arrivals and apply decomposition with the $\tilde{P}_S^+ = 0$-assumption, the retrieved response is overwhelmed by other events as demonstrated in Figure 7d. These are mainly downgoing S-waves since the $\tilde{P}_S^+ = 0$-assumption is not fulfilled in this part of the gather. We conclude that these weak converted waves can not be retrieved without adding information on the shear traction.

Conclusion

Elastic decomposition in boreholes with 4-component receivers is an underdetermined problem. By weighted combinations of geophone and hydrophone recordings, up- and downgoing P-waves can generally be separated, but up- and downgoing S-waves can not. To overcome this problem, we separated up- and downgoing S-waves by time-gating and introduced these separated fields as additional constraints in the decomposition scheme. We tested this approach for multi-component receivers in a deviated well in a complex synthetic model. Up- and downgoing P-waves and downgoing S-waves could be retrieved well. For this model, late upgoing S-wave arrivals could also be retrieved, but earlier converted upgoing S-waves could not. For different configurations, different constraints might be incorporated.

Acknowledgements

This work was supported by the Dutch Technology Foundation STW, applied science division of NWO and the Technology Program of the Ministry of Economic Affairs. We thank Kurang Mehta and Jorge Lopez of Shell E&P Houston for permission to use the elastic model. We thank Jan Thorbecke of Delft University for his help on elastic finite difference modeling.

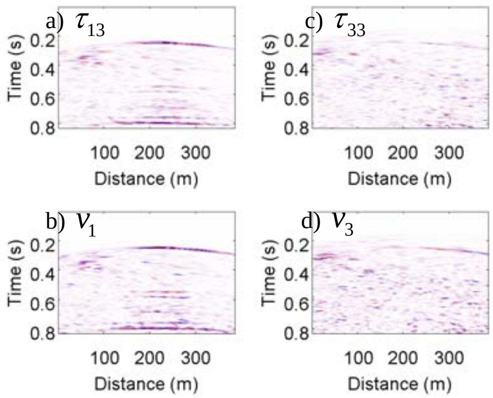

Fig 3: Raw data, horizontal force source: a) shear traction, b) horizontal particle velocity, c) normal traction, d) vertical particle velocity; gain control has been applied.

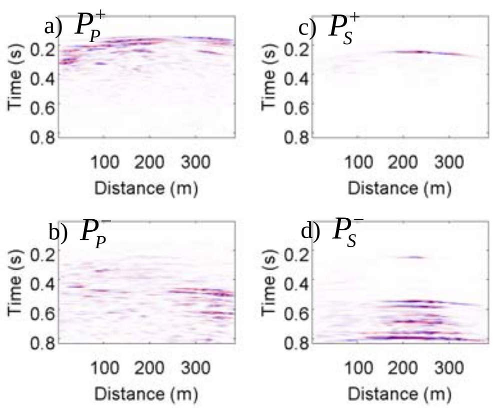

Fig 4: Full decomposition, horizontal force source: a) downgoing P, b) upgoing P, c) downgoing S, d) upgoing S.

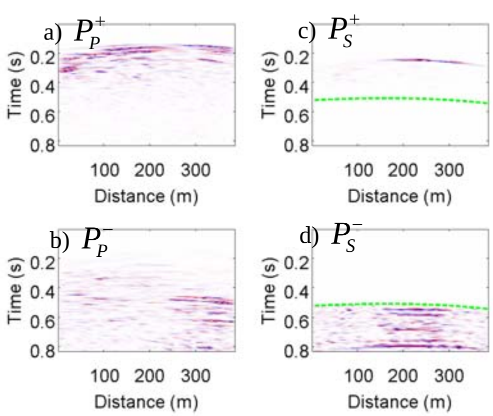

Fig 5: Modified decomposition, horizontal force source: a) downgoing P, b) upgoing P, c) downgoing S, d) upgoing S.

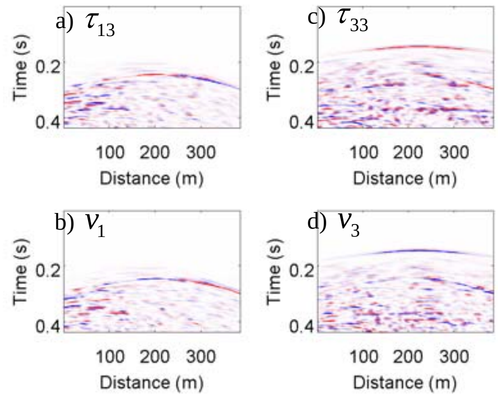

Fig 6: Raw data, vertical force source: a) shear traction, b) horizontal particle velocity, c) normal traction, , d) vertical particle velocity; gain control has been applied.

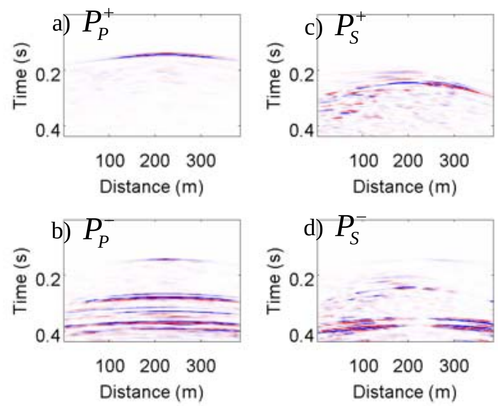

Fig 7: Full decomposition, vertical force source: a) downgoing P, b) upgoing P, c) downgoing S, d) upgoing S.

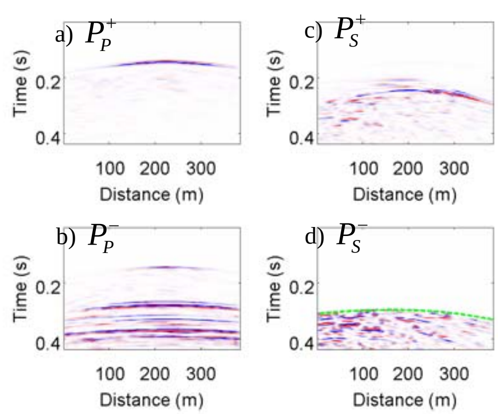

Fig 8: Modified decomposition, vertical force source: a) downgoing P, b) upgoing P, c) downgoing S, d) upgoing S.